

From stretched exponential to power-law: crossover of relaxation in a simple model

Sukanta Mukherjee,^{1,2} Puneet Pareek,¹ Mustansir Barma,^{1,*} and Saroj Kumar Nandi^{1,†}

¹*TIFR Centre for Interdisciplinary Sciences, Tata Institute of Fundamental Research, Hyderabad - 500046, India*

²*Cluster of Excellence Physics of Life, Technische Universität Dresden, Arnoldstraße 18, 01307 Dresden, Germany*

The autocorrelation function in many complex systems shows a crossover of its decay: from stretched exponential relaxation (SER) at short times to power-law at long times. Study of the mechanisms leading to such multiple relaxation patterns are rare. Additionally, the inherent complexity of these systems makes it hard to understand the underlying mechanism leading to the crossover. Here we develop a simple one-dimensional spin model, which we call a Domain Wall to Doublon (DWD) model, that shows such a crossover. The nature of the excitations governing the relaxation dynamics changes with temperature. The relevant excitations are domain walls (DWs) and bound pairs of DWs, which we term “doublons”. The diffusive motions of the DWs govern the relaxation at short times, whereas the diffusive motions of the doublons give the decay at long times. This crossover of relaxation mechanisms leads to the crossover, from SER to power-law, in the decay pattern of the autocorrelation functions. We augment our numerical results by analytical derivations of the relaxation forms.

Relaxation dynamics is fundamental in various branches of science, ranging from the kinetics of reaction rates [1] to diffusion in a complex environment [2] to escape problems [3]. For simple systems, in the absence of disorder or trapping, barrier crossing between valleys leads to exponential relaxation, known as the Maxwell-Debye relaxation [4]. However, the presence of a disorder or spatial heterogeneity leads to a more complex scenario, often resulting in *stretched exponential relaxation (SER)*, as observed in different systems. Examples include dynamics in glasses [5, 6], dielectric relaxation in many organic compounds [7, 8], in systems with arrested steady states [9, 10], etc. It is now well-known that SER can arise from many different mechanisms (see Ref. [10] for a brief overview). For example, Glarum [7] and Bordewijk [11] studied the diffusion dynamics of vacancies in liquid structure to obtain SER. Skinner [8], Spohn [12], Godrèche [13], and others [14] have extended such frameworks to diffusive dynamics of domain walls in spin systems. On the other hand, the relaxation in several complex systems, such as spin glasses below the transition temperature [15, 16], systems close to a critical point [17, 18], stress relaxation in block copolymers [19], are described by even slower decays, characterized by *power laws*.

Most systems generally follow a single relaxation form that describes the decay of the correlation functions. However, there are several systems that show crossovers from one type of decay of the correlation function to another as time progresses. Examples include the dynamics in non-entangled polymeric melts [20], survival kinetics in random walks with fractally correlated traps [21], the ensemble-averaged relaxation process in a model with arrested states [10], the angular-velocity autocorrelation function of an active probe in a glassy medium [22], the self-overlap function in particulate [23] and confluent

biological systems [24, 25], etc. The autocorrelation function in these systems shows a crossover from an SER form to a power law at later times. Although many works have focused on understanding the mechanisms leading to either SER or power law, detailed studies of the dynamics where both these forms are present and the mechanism leading to the crossover are relatively rare.

Metzler and Klafter [26, 27] generalized the standard Markoffian model of diffusive dynamics to fractional dynamics for disordered systems. They demonstrated that relaxations in such systems follow a Mittag-Leffler function, which shows an initial SER followed by a power law at long times. An interesting result in this context is that the stretching exponent, β , of the SER: $C(t) \sim \exp[-(t/\tau)^\beta]$, where t is time and τ is a relaxation time, and the exponent, α , which characterizes the power law: $C(t) \sim (t/\tau)^{-\alpha}$, are the same, that is $\alpha = \beta$. However, there are systems where α and β can differ, for example, the cellular Potts model in 2D [24] or systems with more complexity, as was also hypothesized in Ref. [27]. Whether and how α should be related to β , in general, remains unclear. Since the well-known systems discussed above showing two distinct forms for the decay of the autocorrelation function at different times are complex, it is advantageous for drawing meaningful insights to have simple model systems showing similar dynamical characteristics.

In this work, we define a simple one-dimensional spin model, which we term a Domain Wall to Doublon (DWD) model, to study the crossover of dynamics from SER at short times to a power-law form at long times. The relaxation dynamics is governed by excitations: while at short times, the relevant excitations are individual domain walls (DWs), at long times, the excitations are bound-pairs of DWs that we call “doublons”. The number of DWs in our model is conserved, and there is a hard-core repulsion between them. The short-time dynamics involves the formation of the doublons via the ballistic motion of a pair of DWs toward each other. On the other hand, the long-time dynamics comprises

* barma@tifrh.res.in

† saroj@tifrh.res.in

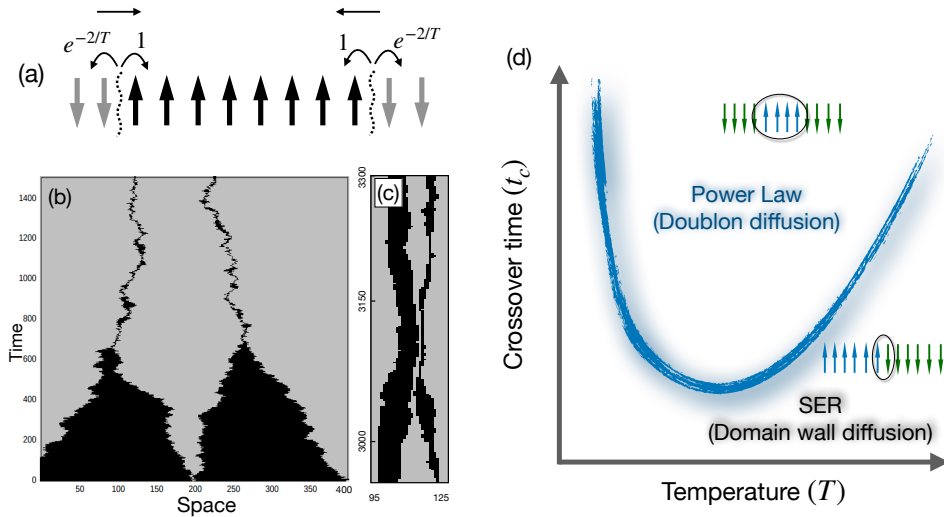


FIG. 1. Basic phenomenology of the dynamics. (a) Consider a domain of \uparrow spins surrounded by \downarrow spins. Due to the energy function, Eq. (1), the probability of flipping a \uparrow spin is 1, whereas that for a \downarrow spin is $e^{-2/T}$. The constraint of the dynamics allows spin-flip only at the boundary of a domain. Thus, the movement of DWs towards the \uparrow spins is favored, as indicated by the arrows. This leads to an effective attractive interaction between DWs separated by \uparrow spins. Such a pair of DWs form a bound state that we term a doublon. (b) Evolution of a system with four DWs, created by two \downarrow spins (marked gray) at equal distances in a system of \uparrow spins (marked black). The system size is 400. The dynamics leads to the formation of two excitations at long times. (c) Hard-core repulsion between two excitations in our simulation. (d) Schematic representation of t_c as a function of T . t_c diverges both for $T \rightarrow 0$ and $T \rightarrow \infty$, for two independent reasons. The crossover time separates the power-law decay from the SER of the autocorrelation function. We emphasize that the crossover time is not sharply defined. The relevant excitations in the two regimes are schematically shown.

the diffusive motion of the doublons. A crossover in the form of the dominant excitation leads to the crossover of the decay pattern of the autocorrelation function. The organization of the rest of the paper is as follows: we introduce the model in Sec. I. For the results, we first present the steady state properties in Sec. II and then the details of the dynamics in Sec. III. We conclude the paper in Sec. IV with a brief discussion of our results.

I. DESCRIPTION OF THE MODEL

Our proposed model is a variant of a specific class known as kinetically constrained models (KCMs). Such models have given crucial insights into the dynamics of glassy systems [14, 28, 29]. They are also relevant to operator spreading and dynamics in quantum many body systems [30, 31], dynamics of Rydberg atoms [32], gravity-driven granular flow and clogging [33], etc. We define a one-dimensional lattice model, where each site i contains an Ising spin $S_i = \pm 1$ and show that the autocorrelation function, characterizing the dynamics, shows a crossover from SER to power-law.

The system is governed by an onsite energy function,

$$\mathcal{H} = \sum_{i=1}^N S_i, \quad (1)$$

where N is the total number of spins. Equation (1)

describes a set of non-interacting spins in a magnetic field of unit strength. The system evolves through single spin-flip Monte-Carlo (MC) dynamics with a kinetic constraint: a spin can flip only if its two nearest neighbors have opposite signs. This latter constraint ensures that the number of DWs remains constant; an allowed spin-flip results in the DW moving one lattice spacing.

It is instructive to compare our model with a couple of other kinetically constrained models which have been studied extensively. At $T = \infty$, the dynamics of our model becomes identical to the energy-conserving dynamics in an Ising spin model with nearest-neighbor interactions [8, 12]. Such dynamics arises, for example, in equilibrium under a sudden quench from a finite T to $T = 0$. The autocorrelation function follows SER with $\beta = 1/2$ in $1D$. If we replace the kinetic constraint in our model with one where spin-flips are allowed only when one of the nearest neighbors is up, the model becomes equivalent to a kinetically constrained model [14, 35]: Depending on whether the spin flip is allowed if the left (or right) neighbor is up, the model is called the East (or West model), respectively. The autocorrelation function follows SER with $\beta = 1/2$ in this case too.

However, there is a difference between these two classes of models: In the first class, total energy and number of DWs are both conserved, whereas, in the second class of models, both can vary. Both result in SER with $\beta = 1/2$. By contrast, in our model, the DW number is conserved,

TABLE I. Comparison of the properties of the three distinct but related models.

Models	Domain Wall Conserved	Energy Conserved	Properties
Energy Conserving Ising Spins	Yes	Yes	SER, $\beta = 1/2$ [12]
East Model	No	No	SER, β is T dependent [14, 34]
DWD Model	Yes	No	Crossover, SER ($\beta = 1/2$) to power law (Exponent = $1/2$) [This work]

whereas the total energy can change, and we find that the autocorrelation function shows a crossover from SER to a power law.

In our simulations, unless otherwise mentioned, we use periodic boundary conditions. The dynamics is as follows: at each step, we choose a spin at random; if the two nearest neighbors of this spin are opposite, we flip the spin with probability $\min(1, \exp[2S_i/T])$. N such attempts provide the unit of time.

Essential characteristics of the model: Before getting into the detailed results, it is instructive to first look into some qualitative aspects of the model. Due to the kinetic constraint, spin flips are allowed only at the interfaces of two domains, i.e., allowed moves involve movements of the DWs. At $T = \infty$, each DW performs a random walk but with a hard-core constraint between DWs. When $T < \infty$, there is a higher flipping rate for a \uparrow spin ($S_i = +1$) than for a \downarrow spin ($S_i = -1$) owing to the applied field. Thus

$$\frac{W(\downarrow \rightarrow \uparrow)}{W(\uparrow \rightarrow \downarrow)} = e^{-2/T} \quad (2)$$

where $W(\uparrow \rightarrow \downarrow)$ is the probability of $\uparrow \rightarrow \downarrow$; we have set the Boltzmann constant, k_B , to unity. Conservation of $\xi = \sum_i S_i S_{i+1} [= (N - 2N_d)]$ leads to different sectors. Within a particular sector, the condition of detailed balance holds. Now, consider a domain of \uparrow spins surrounded by down spins as schematically shown in Fig. 1(a). For any finite value of T , the transition $\uparrow \rightarrow \downarrow$ is more likely than $\downarrow \rightarrow \uparrow$. Therefore, at both ends of a domain, there is a tendency to shrink the \uparrow spin domain, which we can interpret as an effective attractive interaction between the two DWs surrounding each domain of \uparrow spins; the strength of this interaction is maximum at $T = 0$ and vanishes as $T \rightarrow \infty$.

As a result of this effective attractive interaction at $T < \infty$, DWs surrounding \uparrow move towards each other and form a bound state that we define as a “doublon”. Periodic boundary conditions imply an even number, N_d , of DWs. Conservation of DW number is equivalent to the conservation of the number of doublons, given as $N_d/2$. While the minimum size of doublon is one, at finite T the doublon length fluctuates around an average, $\langle \ell \rangle$. The diffusion of the doublons dominates the long-time dynamics. Figure 1(b) shows the evolution of a system with four DWs, created by two \downarrow spins at equal distances in a system of \uparrow spins. The DWs between \uparrow spins move toward each other and form doublons. There is a hard-core repulsion among different doublons; this

comes from the hard-core repulsion among the DWs. Figure 1(c) shows the evolution of two such doublons in our simulation. They move away from each other after coming within one spin apart. Figure 1(d) schematically shows the crossover time, t_c , as a function of T .

II. RESULTS: STATIC PROPERTIES

A. Analytical theory for domain distribution

We first provide analytical results for the static properties in the steady state. For a large enough system size N , we may use a grand canonical description, within which the domain wall number is controlled by a conjugate chemical potential. The grand canonical partition function is

$$\mathcal{Z}(\mu, T) = \sum_{\mathbb{C}} \exp \left[\frac{\mu N_d}{k_B T} \right] \exp \left[-\frac{1}{k_B T} \sum_{i=1}^N S_i \right], \quad (3)$$

where μ is the chemical potential that controls the DW density, k_B is the Boltzmann constant, and \mathbb{C} represents all possible configurations. Since the number of DWs is given by $N_d = \sum_{i=1}^N (1 - S_i S_{i+1})/2$, we obtain

$$\mathcal{Z}(\mu, T) = e^{\frac{\mu N}{2k_B T}} \sum_{\mathbb{C}} e^{-\frac{\mu}{2k_B T} \sum_{i=1}^N S_i S_{i+1} - \frac{1}{k_B T} \sum_{i=1}^N S_i}. \quad (4)$$

Observing that Eq. (4) is just the partition function of the 1D nearest neighbor Ising model, we may use the standard transfer matrix formalism [36] to obtain

$$\mathcal{Z}(\mu, T) = \Lambda_+^N + \Lambda_-^N \quad (5)$$

where

$$\Lambda_{\pm} = \left[\cosh(1/k_B T) \pm \sqrt{z^2 + \sinh^2(1/k_B T)} \right], \quad (6)$$

with $z = \exp[\mu/k_B T]$. For large N , the first term, Λ_+^N , dominates.

Let us define an ℓ -cluster as a stretch of ℓ consecutive up spins, with down spins at the two ends. The probability $P(\ell)$ of the occurrence of an ℓ -cluster is

$$P(\ell) = \langle \downarrow \uparrow \uparrow \dots \uparrow \downarrow \rangle = \langle \bar{n}_i n_{i+1} n_{i+2} \dots n_{i+\ell} \bar{n}_{i+\ell+1} \rangle, \quad (7)$$

where n_i and \bar{n}_i are occupancy variables for \uparrow and \downarrow spins respectively, and are given by

$$n_i = \frac{1 + S_i}{2}; \quad \bar{n}_i = \frac{1 - S_i}{2}. \quad (8)$$

After straight forward algebra, we obtain

$$P(\ell) = C \frac{\exp(-\frac{\ell}{k_B T})}{\left[\cosh(\frac{1}{k_B T}) + \sqrt{z^2 + \sinh^2(\frac{1}{k_B T})} \right]^{\ell+2}}, \quad (9)$$

where C is given as

$$C = \frac{z^4 e^{-\frac{1}{k_B T}} \left[e^{\frac{1}{k_B T}} + \sinh(\frac{1}{k_B T}) + \sqrt{z^2 + \sinh^2(\frac{1}{k_B T})} \right]}{z^2 + \left\{ \sinh(\frac{1}{k_B T}) + \sqrt{z^2 + \sinh^2(\frac{1}{k_B T})} \right\}^2}.$$

Further, the DW density, ρ_{DW} , is given by

$$\rho_{DW} = \frac{\langle N_d \rangle}{N} = \frac{z}{N} \frac{\partial \ln \mathcal{Z}(\mu, T)}{\partial z} \approx \frac{z}{N} \frac{\partial \Lambda_+}{\partial z}. \quad (10)$$

Using Eq. (6), we obtain

$$\rho_{DW} = \frac{z^2}{z^2 + \sinh^2(\frac{1}{k_B T}) + \cosh(\frac{1}{k_B T}) \sqrt{z^2 + \sinh^2(\frac{1}{k_B T})}}. \quad (11)$$

For a given ρ_{DW} , we obtain z using Eq. (11) at a particular T . We then calculate $P(\ell)$ at different T using Eq. (9).

B. Simulation results for steady-state domain distribution

We now present the simulation results for the steady-state doublon length, ℓ , defined as the number of \uparrow spins between two consecutive DWs. We first simulate a system of fixed size with periodic boundary conditions and a certain number of \downarrow spins (each of which creates two DWs) in a system of \uparrow spins. We start with an initial condition where the \downarrow spins are equally spaced; such an initial condition allows the highest possible lengths for the doublons. As the system evolves, ℓ decreases and reaches its equilibrium value. The evolution of the average doublon length, $\langle \ell \rangle$, as a function of time, is shown in Fig. 2(a) for different values of T ; $\langle \ell \rangle$ in equilibrium depends on T . At $T = \infty$, there is no difference between the domains of \uparrow or \downarrow spins, and $\langle \ell \rangle$ is simply the average domain length. $\langle \ell \rangle$ monotonically decreases with decreasing T and becomes unity (one \uparrow spin) at $T = 0$.

In a finite system of size N , with N_d DWs, the maximum $\langle \ell \rangle$ is equal to N/N_d ; this is the saturation value of $\langle \ell \rangle$ at large T , as shown in Fig. 2(b). $\langle \ell \rangle$ decreases with decreasing T and attains the minimum value (one spin) at low enough T , as shown in Fig. 2(b). We have also obtained the theoretical results for $\langle \ell \rangle$ using

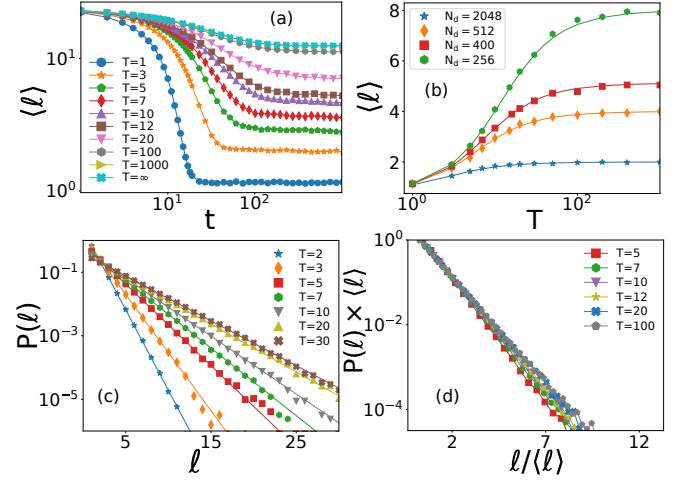


FIG. 2. (a) Evolution of average doublon length, $\langle \ell \rangle$, with 160 equally spaced \downarrow spins and the rest being \uparrow spins with system size $N = 4000$. $\langle \ell \rangle$ attains a T -dependent equilibrium value. Each point is an average of 10^4 systems. (b) Equilibrium behavior of $\langle \ell \rangle$ as a function of T , with $N = 2048$ and different numbers, N_d , of DWs, each point is averaged over 10^4 systems. $\langle \ell \rangle$ saturates to the average domain length, N/N_d , at high T and independent of system size at low T . The lines are theory, and the symbols are simulation data. (c) The distribution of domain lengths, $P(\ell)$, follows an exponential trend. Lines are theory (Eq. 9), and symbols are simulation data. We have used $N = 1024$ and $\rho_{DW} = 0.25$ in the simulations. (d) The plot of the domain length distribution function as a function of $\ell / \langle \ell \rangle$ follows a master curve.

Eq. (9) and show them with the continuous lines in Fig. 2(b); the analytical result agrees well with the simulation data (symbols).

Figure 2(a) shows that $\langle \ell \rangle$ attains a constant value in equilibrium, though the individual values of ℓ fluctuate. Equation (9) shows that ℓ follows a nearly exponential distribution. Figure 2(c) shows $P(\ell)$ at different T ; the lines are theory (Eq. 9), and symbols are simulation data at the corresponding T . Decay of $P(\ell)$ is slower at higher T ; this is natural since $\langle \ell \rangle$ monotonically grows as T increases. To confirm that $P(\ell)$ follows a nearly exponential form, $P(\ell) \sim \exp[-\ell / \langle \ell \rangle]$, we plot $\langle \ell \rangle P(\ell)$ as a function of $\ell / \langle \ell \rangle$ in Fig. 2(d) and find all data follow a master curve as expected.

C. Effects of finite size on the steady-state domain lengths

As shown in Fig. 2(b), $\langle \ell \rangle$ deviates from $\langle \ell \rangle_\infty$ as the system size is finite; we now study these finite-size effects. There are two competing length scales in the system in equilibrium: $\langle \ell \rangle$ and $\rho_{DW}^{-1} = N/N_d$, the inverse of DW concentration. When the number of DWs, N_d , is large, ρ_{DW}^{-1} gives the average domain size, and the equilibrium length $\langle \ell \rangle$ set by T cannot be larger than ρ_{DW}^{-1} . On the other hand, in the limit $\langle \ell \rangle \ll \rho_{DW}^{-1}$, finite-size effects

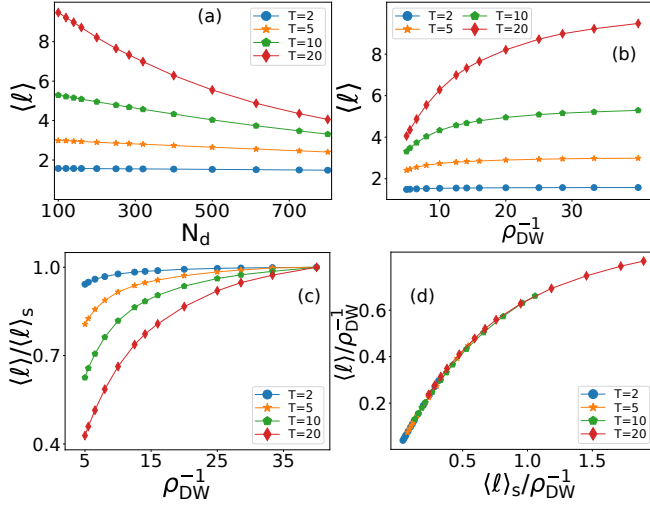


FIG. 3. (a) Average length, $\langle \ell \rangle$, of doublons in equilibrium as a function of N_d . (b) $\langle \ell \rangle$ as a function of ρ_{DW}^{-1} . $\langle \ell \rangle$ saturates to a T -dependent value, $\langle \ell \rangle_s$, when ρ_{DW}^{-1} is large. (c) $\langle \ell \rangle / \langle \ell \rangle_s$ is shown as a function of ρ_{DW}^{-1} . (d) The plot of $\langle \ell \rangle / \rho_{DW}^{-1}$ as a function of $\langle \ell \rangle_s / \rho_{DW}^{-1}$ follows a master curve for data at different T , confirming our finite-size scaling ansatz, Eq. (12). System size $N = 4000$ for all the simulation data presented in this figure. Each point represents an average of 10^4 systems.

in $\langle \ell \rangle$ are not relevant. To study this effect, we place N_d number of DWs in a system of size N and study $\langle \ell \rangle$ with varying N_d at different T . Figure 3(a) shows $\langle \ell \rangle$ at four values of T as a function of N_d , $\langle \ell \rangle$ decreases with increasing N_d . Figure 3(b) shows $\langle \ell \rangle$ as a function of ρ_{DW}^{-1} ; as evident from the plot, $\langle \ell \rangle$ saturates to a T -dependent value when ρ_{DW}^{-1} is large enough. As this saturation value of $\langle \ell \rangle$, denoted as $\langle \ell \rangle_s$, depends on T , we find larger $\langle \ell \rangle_s$ at higher T . Plot of $\langle \ell \rangle / \langle \ell \rangle_s$ as a function of ρ_{DW}^{-1} , as presented in Fig. 3(c), shows the approach to saturation depends on T , which can be characterized in terms of $\langle \ell \rangle_s$.

To summarize these observations, we propose the following form for $\langle \ell \rangle$:

$$\langle \ell \rangle = \rho_{DW}^{-1} \mathcal{F}(\langle \ell \rangle_s / \rho_{DW}^{-1}), \quad (12)$$

with the function $\mathcal{F}(x)$ having the following properties

$$\mathcal{F} = \begin{cases} x, & \text{when } x \rightarrow 0 \\ 1, & \text{when } x \rightarrow \infty. \end{cases} \quad (13)$$

Therefore, the plot of $\langle \ell \rangle / \rho_{DW}^{-1}$ as a function of $\langle \ell \rangle_s / \rho_{DW}^{-1}$ for different sets of data should follow a master curve. The data collapse, shown in Fig. 3(d), is thus consistent with our ansatz, Eq. (12).

III. RESULTS: DYNAMICAL PROPERTIES

We now study the dynamical properties of the system, starting from a random state. As discussed in the

previous section, there exists a bias of DW movement, it tries to minimise the number of \uparrow spins. The presence of this bias will lead to ballistic dynamics at finite T . To test this, we consider a system of fixed size $l + 1$, where the left-most spin is \downarrow , and the rest of them are \uparrow . We do *not* impose periodic boundary conditions for these simulations and calculate the mean-first passage time, $MFPT(l)$, defined as the average time when the l th spin gets flipped for the first time. $MFPT(l)$ varies as l^2 for purely diffusive dynamics, and it varies linearly with l when the dynamics is ballistic. We find that $MFPT(l)$ indeed linearly depends on l , as shown in Fig. 4(a) at different T .

The energy function, Eq. (1), gives the rate of $\downarrow \rightarrow \uparrow$ spin-flip as $\exp[-2/T]$, while the rate of $\uparrow \rightarrow \downarrow$ is unity. Then, on average, the probability per unit time that a DW moves right, gives the velocity, $v = (1 - \exp[-2/T])$. We obtain v in simulation as the inverse of the slopes of $MFPT(l)$, as presented in Fig. 4(a). The simulation data for v , as shown by symbols in Fig. 4(b), and the continuous line representing $1 - \exp[-2/T]$ agree well. As v gives the average velocity of the DW, $MFPT(l)$ is l/v . Thus, the plot of $MFPT(l)$ as a function of l/v should follow a master curve with slope unity, as confirmed by the simulation data [inset of Fig. 4(b)].

A. Autocorrelation function

We now study the dynamics and show that relaxation at short times can be understood via the dynamics of individual DWs, while the long-time relaxation involves the diffusion of doublons. We characterize the relaxation dynamics through the autocorrelation function, $C(t)$, defined as

$$C(t) = \overline{\left\langle \frac{1}{N} \sum_{i=1}^N S_i(t_0) S_i(t_0 + t) \right\rangle_{t_0}} - \sigma^2, \quad (14)$$

where σ is the average equilibrium magnetization. $\langle \dots \rangle_{t_0}$ and the overline define averages over the initial time t_0 and initial configurations, respectively.

We show the behavior of $C(t)$ at $T = 1$ with different numbers of DWs in Fig. 4(c) and with a fixed number of DWs, $N_d = 172$, at various T in Fig. 4(d). The two distinct types of decay are apparent from the figures: the short-time decay is stretched exponential, $\exp[-(t/\tau)^\beta]$ with $\beta = 1/2$, and the long-time behavior follows a power law, $t^{-1/2}$; the fits to these specific functions are shown in Fig. 4(e). As discussed earlier, the $T = \infty$ limit of the system is equivalent to the diffusive dynamics of DWs [8, 12], and $C(t)$ decays via SER. At finite T , there is a tendency of the DWs to move inwards into an \uparrow spin cluster. However, this bias is negligible at very short times, and the DWs dynamics is diffusive; hence, the infinite T mechanism dominates. The cross-over time, t_c , between the SER and the power-law decay seems non-monotonic with T , as shown in Fig. 4(f). t_c decreases

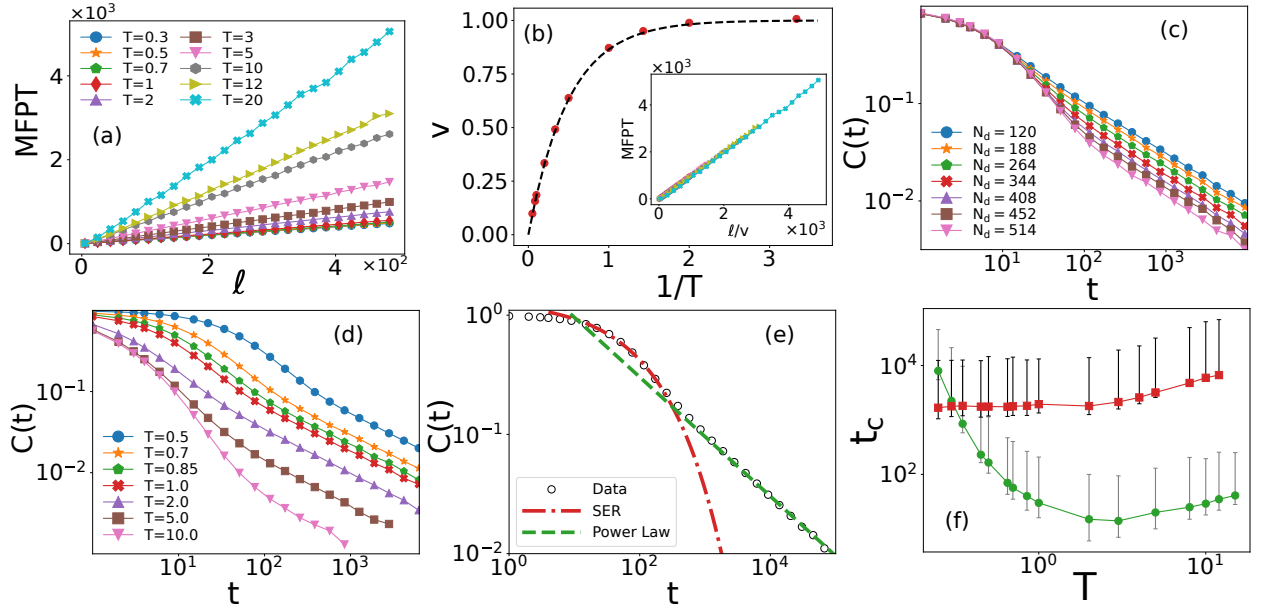


FIG. 4. (a) Mean first-passage time, $MFPT(l)$ as a function of domain length l follows a straight line, showing the ballistic dynamics of DWs. (b) Domain wall velocity, v as a function of inverse T follow $v = 1 - \exp(-2/T)$, symbols are simulation data, and the line is the function. **Inset:** The plot of $MFPT(l)$ as a function of l/v follows a master curve. (c) Decay of the autocorrelation function, $C(t)$ [Eq. (14)], for different numbers, N_d , of DWs at $T = 1$. (d) $C(t)$ as a function of t at different T and $N_d = 344$. (e) Decay of $C(t)$ shows two different regimes: it follows an SER at short t , the fitted function is $f(t) \sim \exp[-(t/\tau)^{1/2}]$, and a power-law at long times, the fitted function is $f(t) \sim t^{-1/2}$. (f) The crossover-time, t_c , shows a non-monotonic trend as most MC attempts are unsuccessful at low T . The trend becomes monotonic when we define time via the accepted moves alone. The error bars represent an estimate of the uncertainty in evaluating t_c . [$N = 1024$ for Figs. (d)-(f)].

with decreasing T till a particular T and then increases below it. Note that many possible moves are unsuccessful at low T : this affects the time scale of the dynamics. Interestingly, when we define units of time as N number of accepted moves, we find a monotonic behavior for t_c , as shown in Fig. 4(f). Thus, the non-monotonic behavior has its origin in the rejected moves of MC dynamics at low T .

B. Analytical arguments for the crossover of autocorrelation function

We now discuss the mechanisms leading to the crossover in the relaxation dynamics. The DW dynamics is faster than the doublon dynamics. Since the bias is appreciable only on average, the DWs will move diffusively at short times when the bias is negligible. The bias becomes significant only at long times, and the pair of DWs, i.e., the doublons, move diffusively. Thus, at short times, $t \ll t_c$, the diffusive motion of DWs governs the decay of $C(t)$: this is the mechanism of relaxation proposed by Spohn [12]. At this time scale, we can write down the time-dependence of the autocorrelation

function as

$$C(t) = \sum_l P(l) e^{-t/Al^2} \sim \sum_l e^{-[l/\langle \ell \rangle + t/Al^2]} \quad (15)$$

where A is related to the diffusivity of the DWs. The time taken for relaxation of a domain of size l is t , thus, $l^2 \propto t$, and we obtain from the above,

$$C(t) \sim e^{-\sqrt{t}/\langle \ell \rangle} \quad (16)$$

leading to the SER relaxation at short times.

On the other hand, at a time-scale $t \sim t_c$, the bias in the DW movement is significant, and a pair of DWs can move as a bound state in the form of a doublon; further relaxation of the system can only occur via the dynamics of the doublons. We now analytically show that the diffusive dynamics of the doublons leads to a power-law relaxation. The number of doublons in our system is constant and equals $N_d/2$. The hard-core repulsion of DWs implies that the doublons too cannot cross each other. Therefore, on large enough length and timescales we can study the doublon dynamics by treating them as hard-core particles in the system. As detailed in Ref. [37] and discussed in brief below, we can map the dynamics of such a system to that of a Heisenberg model.

Consider a system size of N with n doublons in it. The occupancy number n_i of a site i is τ_i^z as $n_i = (1 + \tau_i^z)/2$,

where τ_i^x , τ_i^y , and τ_i^z are the x , y , and z components of the Heisenberg spin variable $\boldsymbol{\tau}_i$. Consideration of the hard-core nature of the particles and the fact that there can not be any dynamics between two empty sites, the dynamics with rate u , in an infinitesimal time, dt , between two sites i and j , can be written in terms of the time-evolution operator U_{dt}^{ij} , defined as,

$$U_{dt}^{ij} = 1 - \frac{udt}{2}[1 - 4\boldsymbol{\tau}_i \cdot \boldsymbol{\tau}_j] \simeq e^{-\frac{udt}{2}[1 - 4\boldsymbol{\tau}_i \cdot \boldsymbol{\tau}_j]}. \quad (17)$$

Thus, the evolution operator for the entire system, for a finite time t , can be written as $U_t = \exp[-\frac{ut}{2} \sum_{\langle ij \rangle} (1 - 4\boldsymbol{\tau}_i \cdot \boldsymbol{\tau}_j)]$ and the mapping is complete with the identification of the Hamiltonian of the Heisenberg model $\mathcal{H} = \frac{u}{2} \sum_{\langle ij \rangle} (1 - 4\boldsymbol{\tau}_i \cdot \boldsymbol{\tau}_j)$. Let $|k\rangle$ be the eigenstate of \mathcal{H} with energy ε_k and $|G_r\rangle$ is the ground state in the sector with r down spins, then the correlation function can be written as [37]

$$C_{ij}(t) = \langle n_i(t)n_j(0) \rangle - \langle n_i(t) \rangle \langle n_j(0) \rangle = \frac{1}{4} \sum_{k \neq G_r} e^{-\varepsilon_k t} \langle G_r | \tau_i^z | k \rangle \langle k | \tau_j^z | G_r \rangle. \quad (18)$$

From the above form, it is clear that the autocorrelation function is determined by the exponential part alone as the rest in Eq. (18) gives a time-independent contribution. From \mathcal{H} , we obtain $\varepsilon_k = 2u(1 - \cos k)$ [37]. Since the energy appears in the exponential, we take the small k -expansion of the cosine and obtain $C(t)$ as

$$C(t) \equiv C_{ii}(t) = \mathcal{B} \int e^{-uk^2 t} dk = \mathcal{B} \sqrt{\frac{\pi}{4ut}}, \quad (19)$$

where \mathcal{B} is the t -independent part in Eq. 18. Thus, $C(t)$ is expected to decay as $t^{-1/2}$ at all T and N_d ; this agrees well with the numerical results presented in Fig. 4.

IV. DISCUSSION AND CONCLUSION

The crossover of different forms of the autocorrelation function generally signifies a change of mechanisms operating at various times. Such crossover scenarios are ubiquitous in many complex systems [10, 20, 26, 27], particularly in biological systems, where relaxation dynamics can have additional nontrivial contributions from activity [22, 24]. The study of the mechanisms leading to such crossover is relatively rare compared to systems following single relaxation functions. In this work, we have studied such a mechanism within a simple one-dimensional model, which we call DWD model. The model falls under the broad category of kinetically constrained models. The kinetic constraint that a spin can only flip when two of its nearest neighbors are opposite. Along with the on-site potential energy, this leads to a surprisingly rich behavior. At short

times, the system relaxes due to the ballistic and diffusive motion of the domain walls. The mechanism changes at long times when the system relaxes via the diffusive motion of doublons, which are comprised of a number of up spins between two DWs. In the steady state, the length of the doublons varies exponentially. Since ballistic dynamics is faster than diffusive dynamics, the former dominates at short times and the latter at long times.

The simplicity of our model allows us a detailed characterization of the mechanism and an analytical derivation for the decay of the autocorrelation function. The $T = \infty$ limit of the model becomes the same as the energy-conserving dynamics in an Ising model under a rapid quench to zero temperature that shows SER. The SER behavior at short times in our model has an identical mechanism as the bias is applicable on the average and appreciable over a longer time. Our analytical derivation for the power-law relaxation is generic and applies to the diffusive dynamics of a conserved number of particles or doublons. In a recent work, some of us have shown that the overlap function $Q(t)$, characterizing the relaxation dynamics of glassy systems, shows a similar crossover from SER at short times to power law at long times [23]. The long-time power-law behavior of $Q(t)$ is $Q(t) \sim t^{-d/2}$, where d is the dimension, which is similar to the current problem. However, the SER behavior is different: whereas the stretching exponent in the current model remains constant, that for $Q(t)$ depends on T . It will be interesting to explore if we can relate the dynamics of the doublons to that of the cooperatively rearranging regions.

The crossover of relaxation functions reported to date seems to be SER at short times and power-law at long times [10, 20–22, 24]. The framework of Ref. [27] seems to suggest that the crossover between these two functions might be predominant as they both can be described through the Mittag-Leffler function. However, the mechanism reported there stems from the fractional dynamics in systems in the presence of disorder.

On the other hand, Ref. [21] presented a crossover resulting from fractally correlated traps. Interestingly, a crossover of relaxation forms - from SER to power-law - can appear from the ensemble average of local relaxation functions with varying relaxation times.

Ref. [10] studied the spin model with nearest and next-nearest neighbor interaction via the double-spin flip dynamics, where pairs of adjacent parallel spins are flipped at a time with some rules. The dynamics conserves the total number of DWs. For a given initial condition, the number of DWs is constant. The autocorrelation function follows an SER, and the relaxation time depends on the number of DWs. However, when we take an average over the initial conditions, the resulting autocorrelation function shows a crossover from SER to a power law; this contrasts with the mechanism studied in the current work. It is well-known that SER can arise from several distinct processes [10]; therefore, it seems

natural that such a crossover can also come from different mechanisms. In the current model, such a crossover

comes from the distinct natures of the excitations involved in the relaxation dynamics at short and long times.

-
- [1] G. H. Weiss, E. A. DiMarzio, and R. J. Gaylord, *J. Stat. Phys.* **42**, 567 (1986).
 - [2] P. Hänggi, P. Talkner, and M. Borkovec, *Rev. Mod. Phys.* **62**, 251 (1990).
 - [3] H. A. Kramers, *Physica* **7**, 284 (1940).
 - [4] J. C. Maxwell, *Phil. Trans. Royal Soc.* **157**, 49 (1867).
 - [5] L. Berthier and G. Biroli, *Rev. Mod. Phys.* **83**, 587 (2011).
 - [6] J. C. Phillips, *Rep. Prog. Phys.* **59**, 1133 (1996).
 - [7] S. H. Glarum, *J. Chem. Phys.* **33**, 639 (1960).
 - [8] J. L. Skinner, *J. Chem. Phys.* **79**, 1955 (1983).
 - [9] D. Das and M. Barma, *Phys. Rev. E* **60**, 2577 (1999).
 - [10] V. Gupta, S. K. Nandi, and M. Barma, *Phys. Rev. E* **102**, 022103 (2020).
 - [11] P. Bordewijk, *Chem. Phys. Lett.* **32**, 592 (1975).
 - [12] H. Spohn, *Communications in Mathematical Physics* **125**, 3 (1989).
 - [13] C. Godrèche and J. M. Luck, *J. Stat. Mech.*, P05033 (2015).
 - [14] F. Ritort and P. Sollich, *Adv. in Phys.* **52**, 219 (2003).
 - [15] D. E. MacLaughlin, L. C. Gupta, D. W. Cooke, R. H. Heffner, M. Leon, and M. E. Schillaci, *Phys. Rev. Lett.* **51**, 927 (1983).
 - [16] A. Keren, P. Mendels, I. A. Campbell, and J. Lord, *Phys. Rev. Lett.* **77**, 1386 (1996).
 - [17] P. M. Chaikin and T. C. Lubensky, *Principles of Condensed Matter Physics* (Cambridge University Press).
 - [18] H. E. Stanley, *Introduction to Phase Transitions and Critical Phenomena* (Oxford University Press, 1997).
 - [19] M. Rubinstein and S. P. Obukhov, *Macromolecules* **26**, 1740 (1993).
 - [20] F. Ganazzoli, G. Raffainia, and V. Arrighi, *Phys. Chem. Chem. Phys.* **4**, 3734 (2002).
 - [21] D. Plyukhin and A. V. Plyukhin, *Phys. Rev. E* **94**, 042132 (2016).
 - [22] C. Abaurrea-Velasco, C. Lozano, C. Bechinger, and J. de Graaf, *Phys. Rev. Lett.* **125**, 258002 (2020).
 - [23] P. Pareek, M. Adhikari, C. Dasgupta, and S. K. Nandi, *arXiv*, [arXiv:2305.18042](#) (2023).
 - [24] S. Sadhukhan and S. K. Nandi, *Phys. Rev. E* **103**, 062403 (2021).
 - [25] S. Pandey, S. Kolya, S. Sadhukhan, and S. K. Nandi, *arXiv*, [arXiv:2306.07250](#) (2023).
 - [26] R. Metzler and J. Klafter, *Chem. Phys. Lett.* **321**, 238 (2000).
 - [27] R. Metzler and J. Klafter, *J. Non-Crystall. Solids* **305**, 81 (2002).
 - [28] J. P. Garrahan and D. Chandler, *Phys. Rev. Lett.* **89**, 035704 (2002).
 - [29] S. Katira, J. P. Garrahan, and K. K. Mandadapu, *Phys. Rev. Lett.* **123**, 100602 (2019).
 - [30] A. Nahum, J. Ruhman, S. Vijay, and J. Haah, *Phys. Rev. X* **7**, 031016 (2017).
 - [31] M. C. Bañuls and J. P. Garrahan, *Phys. Rev. Lett.* **123**, 200601 (2019).
 - [32] I. Lesanovsky and J. P. Garrahan, *Phys. Rev. Lett.* **111**, 215305 (2013).
 - [33] G. Bolshak, R. Chatterjee, R. Lieberman, and Y. Shokef, *Phys. Rev. E* **100**, 032137 (2019).
 - [34] P. Sollich and M. R. Evans, *Phys. Rev. E* **68**, 031504 (2003).
 - [35] A. Crisanti, F. Ritort, A. Rocco, and M. Sellitto, *J. Chem. Phys.* **113**, 10615 (2000).
 - [36] R. K. Pathria, *Statistical Mechanics*, 2nd ed. (Butterworth Heinemann, 1996).
 - [37] R. B. Stinchcombe, M. D. Grynberg, and M. Barma, *Phys. Rev. E* **47**, 4018 (1993).